Scientific Research Publishing

Open Journal of Geology, 2019, 9, 474-496
http://www.scirp.org/journal/ojg
ISSN Online: 2161-7589
ISSN Print: 2161-7570

Baddeleyite from Large Complex Deposits: Significance for Archean-Paleozoic Plume Processes in the Arctic Region (NE Fennoscandian Shield) Based on U-Pb (ID-TIMS) and LA-ICP-MS Data

Tamara Bayanova[1*], Viktor Subbotin[1], Svetlana Drogobuzhskaya[2], Anatoliy Nikolaev[2], Ekaterina Steshenko[1]

[1]Geological Institute, Kola Science Centre, Russian Academy of Sciences, Apatity, Russia
[2]Tananaev Institute of Chemistry, Kola Science Centre, Russian Academy of Sciences, Apatity, Russia
Email: *tamara@geoksc.apatity.ru, steshenko@geoksc.apatity.ru, drogo_sv@chemy.kolasc.net.ru

How to cite this paper: Bayanova, T., Subbotin, V., Drogobuzhskaya, S., Nikolaev, A. and Steshenko, E. (2019) Baddeleyite from Large Complex Deposits: Significance for Archean-Paleozoic Plume Processes in the Arctic Region (NE Fennoscandian Shield) Based on U-Pb (ID-TIMS) and LA-ICP-MS Data. *Open Journal of Geology*, **9**, 474-496.
https://doi.org/10.4236/ojg.2019.98031

Received: June 25, 2019
Accepted: August 27, 2019
Published: August 30, 2019

Abstract

Baddeleyite is an important mineral geochronometer. It is valued in the U-Pb (ID-TIMS) geochronology more than zircon because of its magmatic origin, while zircon can be metamorphic, hydrothermal or occur as xenocrysts. Detailed mineralogical (BSE, KL, etc.) research of baddeleyite started in the Fennoscandian Shield in the 1990s. The mineral was first extracted from the Paleozoic Kovdor deposit, the second-biggest baddeleyite deposit in the world after Phalaborwa (2.1 Ga), South Africa. The mineral was successfully introduced into the U-Pb systematics. This study provides new U-Pb and LA-ICP-MS data on Archean Ti-Mgt and BIF deposits, Paleoproterozoic layered PGE intrusions with Pt-Pd and Cu-Ni reefs and Paleozoic complex deposits (baddeleyite, apatite, foscorite ores, etc.) in the NE Fennoscandian Shield. Data on concentrations of REE in baddeleyite and temperature of the U-Pb systematics closure are also provided. It is shown that baddeleyite plays an important role in the geological history of the Earth, in particular, in the break-up of supercontinents.

Keywords

Baddeleyite, PGE, U-Pb Isotope Data, Geochronology, Paleoproterozoic PGE Layered Intrusion, Complex Deposits, Paleozoic, Fennoscandian Shield

1. Introduction

Baddeleyite, or zirconium dioxide (ZrO_2), was discovered in Sri Lanka (Ceylon)

more than 100 years ago. It was found by tea magnate Joseph Baddeley and called after him [1]. The mineral occurs in numerous terrestrial and lunar rocks [1]. Just like zircon, it was first studied using U-Pb isotope analysis only in the 1990s by T. Krogh and his associates F. Corfu, S. Kamo, L. Heaman and others. In U-Pb studies with the isotope dilution-thermal ionization mass spectrometry (ID-TIMS) and precise dating of reference complexes, baddeleyite benefits from its best-preserved U-Pb isotope systematics, high concentrations of U and Pb and a low discordance degree, compared to zircon. However, it is difficult to separate baddeleyite because of its minor amounts in silica-undersaturated rocks: gabbro, anorthosites, carbonatites, diabase dikes, etc. Besides, concentrations of baddeleyite are lower and findings are fewer than those of zircon [1] [2] [3]. First publications on the REE distribution in baddeleyite are provided by [4] for Phalaborwa deposit (South Africa).

The purpose of this work is 1) to study the distribution and concentrations of rare earth elements (REE) in baddeleyite, using the laser ablation inductively coupled plasma (LA-ICP-MS) mass spectrometry (ELAN 9000 DRC-e mass spectrometer), and 2) to estimate the precise age of the U-Pb system closure using ID-TIMS and crystallization temperatures of baddeleyite compared to zircon from Neoarchean Ti-Mgt and BIF deposits, than Paleoproterozoic Co-Cu-Ni, Ti-Cr-V-Mgt, Pt-Pd layered intrusions and Paleozoic complex deposits of the NE Fennoscandian Shield.

The paper presents a novel technique of estimating concentrations and distribution of REE in samples from major deposits of the NE Fennoscandian Shield and provides important information on REE contents in the studied objects.

For the first time, this paper provides a modeled link between the break-up of supercontinents and complex deposits with baddeleyite, since all complex deposits are derivates of LIPs from the Archean to Paleozoic.

2. Materials and Methods

The NE Fennoscandian (Baltic) Shield (**Figure 1**) is composed of grey and tonalite-trondhjemite gneisses (TTG) in the Paleoarchean Murmansk (I) and Central Kola (II) megablocks [5]. Recently, cores of single zircon grains from high aluminous gneisses of the Central Kola megablock near Murmansk have been dated at 3.7 Ga, using the SHRIMP-II technique [6]. According to [7], 35 age estimates of the world-oldest zircons had been obtained by 2003. Later on, the 36th age has been estimated for zircon in TTG from Syria (Finland) [8]. The age reported in [6] is the 37th "piece" in the "Late Archean record puzzle" [7].

The Neoarchean Kolmozero-Voronja (III) Greenstone Belt divides the Murmansk and Central Kola megablocks. The latter hosts the largest BIF deposits of Olenegorsk (1) and Kirovogorsk (with U-Pb on baddeleyite from Neoarhaean dikes) [9].

The Keivy terraine (IV) contains Neoarhaean alkaline granite [10] [11] and

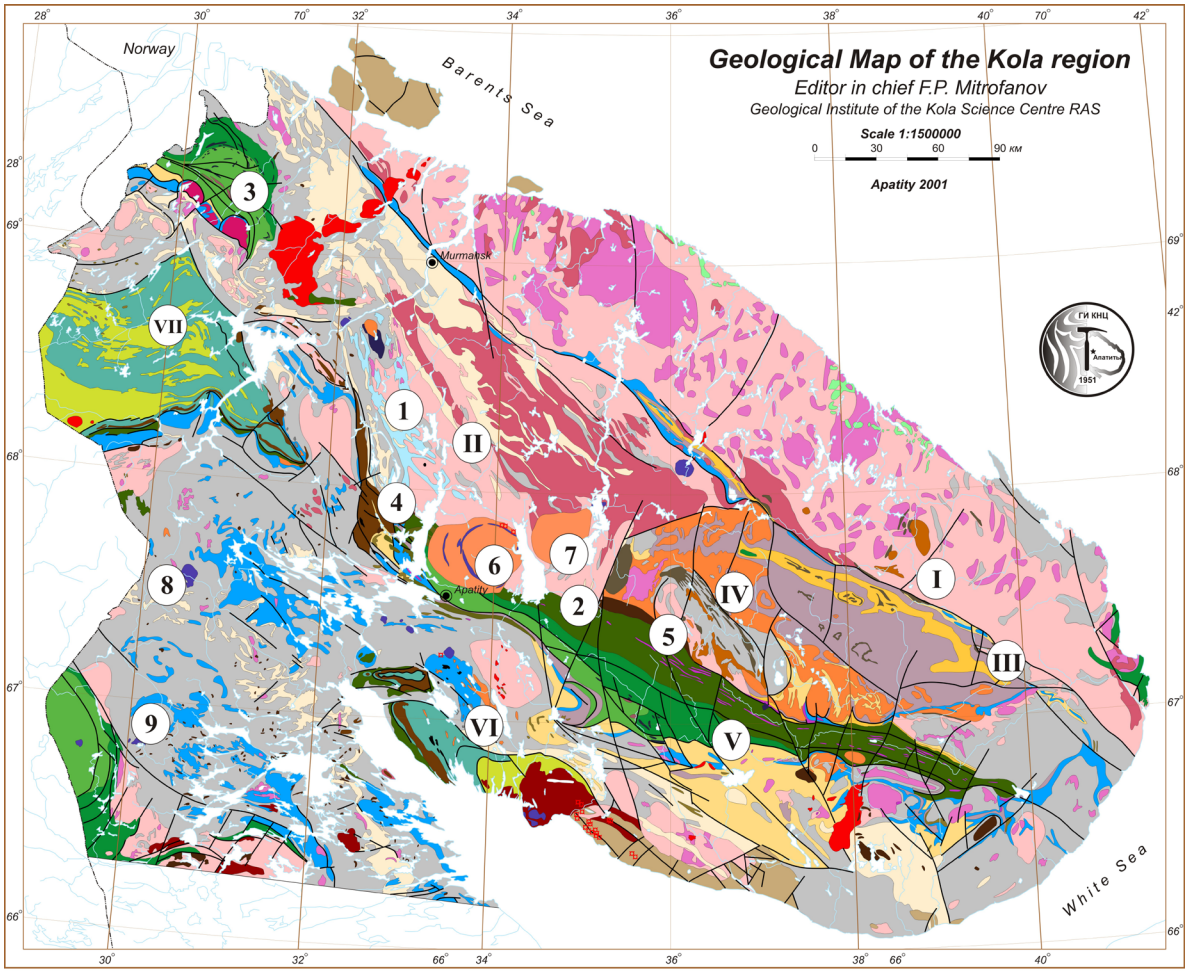

Figure 1. Geological map of the Kola region (modified after [16]).

Ti-Mgt Tsaga (2) deposits. They have been U-Pb dated as Neoarchean [12]. For the first time, the U-Pb method has been applied to date baddeleyite from carbonatites [12] in the Siilinjarvi deposit (Finland) [13].

Besides, the Central Kola megablock comprises superlarge Proterozoic Cu-Ni deposits, *i.e.* the Pechenga (3), Monchegorsk (4) and Fedorovo-Pana (5) ore areas with Pt-Pd, Cr and Pt-Pd reefs and major deposits. This megablock also hosts the superlarge Paleozoic Khibiny (6) and Lovozero (7) massifs with complex foscorite-apatite-nepheline ores.

The NE Fennoscandian Shield is the second-biggest PGE-bearing province in Russia after the Norilsk (**Figure 1**) ore area [14]. It is commercially important owing to Co-Cu-Ni (Monchegorsk area), Cr-Ti-Fe-V (Imandra lopolith) and low-sulfide Pt-Pd ores with Au + Aq (Fedorovo-Pana complex) [14].

The Paleoproterozoic Pechenga-Imandra-Varzuga Greenstone Belt (V) separates the Central Kola megablock from the Belomorian belt, which is a thick subduction zone [15]. This complex terrain includes giant deposits of the ring-like Paleozoic Kovdor (8) and Vuorijarvi intrusions (9). The Lapland Paleoproterozoic granulite belt (VII) is located in the southern part of the Pechenga structure [5] [16].

Baddeleyite has been sampled from Archean to Paleozoic deposits in the north-eastern part of the Fennoscandian Shield (**Figure 1**). It has been separated from a 50 - 100 kg reference sample using the technique described in [3] [13] [17].

Isotope U-Pb (ID-TIMS) studies have been performed using a 7-channel mass spectrometer Finnigan-MAT 262 with a quadrupole RPQ, following the technique with ^{208}Pb and ^{205}Pb tracers suggested in [3] [17]. LA-ICP-MS has been adjusted to study concentrations and distribution of REE in baddeleyite only recently [4] [18] [19].

A new technique of estimating concentrations and distribution of REE in samples using LA-ICP-MS (ELAN 9000 DRC-e, UP 266 MAKRO) has been applied in the Tananaev Institute of Chemistry KSC RAS (Apatity, Russia) to study REE in zircon crystals [20]. Microprobe analyses of resin-mounted samples have been carried out using LEO-1415. Analytical points have been selected on baddeleyite crystals based on analyses of their BSE and CL-images (LEO-1415), as well as optic images (LEICA OM 2500 P, camera DFC 290). Trace and REE analyses of baddeleyite crystals have been carried out *in situ* on polished thin sections by laser ablation inductively coupled plasma mass spectrometry, using a Perkin Elmer ELAN 9000 DRC-e quadrupole mass spectrometer equipped with a 266 nm UP-266 MACRO laser (New Wave Research).

Experiments have been carried out using argon with a repetition rate of 10 Hz, pulse duration of 4 ns, energy density of 14 - 15 J/cm^2 at a spot with a diameter of 35 - 100 μm. External calibration was carried out using NIST 612 glass with the known concentration of REE, U, Th of 40 ppm as a multi-point calibration forced through the origin after blank correction. A diameter of the laser beam has been changed, while all of the rest parameters were stable: from 35 to 240 μm

(r = 0.999). Sample NIST SRM 610 with the concentration of 450 ppm has been used to check the accuracy of estimations [20] [21] [22]. The NIST SRM 610 and NIST SRM 612 [23] [24] [25] glasses are silicate glass reference materials produced by the National Institute of Standards and Technology. Considering calibration standards, measurements of the elements are within the range of 15% relative deviations. The precision was typically 15% RSD for all isotopes after internal correction of diameter of the laser beam. The determination limits are in the range of 0.01 ppm, when a diameter of the laser beam is 155 μm. It complies with the available data [4] [18] [19]. The results have been verified in inter-laboratory cross-checks and analyses of internationally approved standard zircon samples 91500, TEMORA 1 and Mud Tank [20] [21] [22].

3. Results

3.1. Baddeleyite in Neoarchean BIF and Ti-Mgt Deposits

The Neoarchean BIF (Kirovogorskoye), It-Mgt (Tsaga) and zircon (Siilinjarvi) deposits have been dated using the classic U-Pb analysis on zircon and baddeleyite (**Figure 2**, **Table 1**).

LA-ICP-MS has been applied to study zircons from dike rocks that intersect the Olenegorsk BIF, comprising the Kirovogorskoye deposit. **Figure 3**, **Table 2** and **Table 3** provide data on concentrations and distribution of REE in the Kirovogorskoye deposit. Temperatures of the zircon crystallization and closure of the U-Pb systematics have been estimated (**Table 4**) according to [27].

Spectra of REE distribution in zircon crystals show minor amount of LREE and major amount of heavy REE. It explains a steep positive incline of the graphs complicated by negative Eu anomalies and positive Ce anomalies, which complies with the trend of the REE distribution in zircon grains of the magmatic origin (**Figure 3**).

Gabbronorites intersecting the Kirovogorskoye deposit of the Olenegorsk BIF have been studied using LA-ICP-MS. This method has been applied to study zircons of 3 morphotypes with an average total amount of REE from 826 to 1099 ppm (**Table 2**). Since LREE are minor, values of $(La/Yb)_N$ are low (0.000337 -

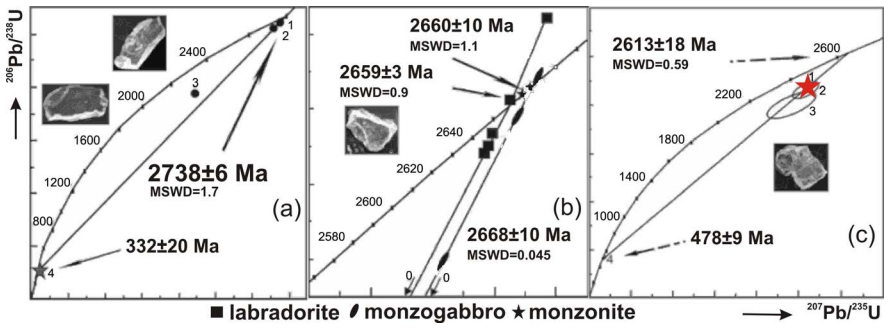

Figure 2. (a) U-Pb diagram for zircon (1 - 3) and baddeleyite (4) from a dike of basic rocks, Kirovogorskoye Fe deposit; (b) U-Pb for zircon and baddeleyite from different rocks, Tsaga Ti-Mgt deposit; (c) U-Pb for baddeleyite (1) and zircon (2 - 4), Siilinjarvi (collection of A. Silvennoinen, Finland).

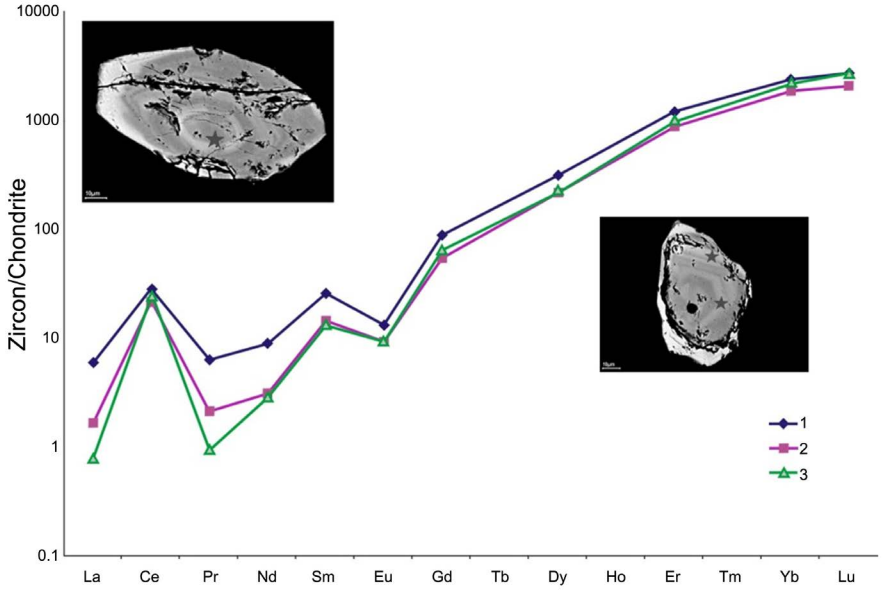

Figure 3. Distribution of REE in zircon from a gabbronorite dike intersecting the Kirovogorskoye Fe deposit [28].

Table 1. U-Pb isotope data on baddeleyite (bd) and zircon from: gabbronorite dike at the Kirovogorskoye deposit (1); Siilinjarvi carbonatites (2); Tsaga massif, monzogabbro (3); Tsaga massif, labradorite (4); Borehole C-1, monzonite (5).

Sample No.	Weight mg	Concentration (ppm)		Pb isotope composition[1]			Isotope ratios[2]			Rho
		Pb	U	$^{206}Pb/^{204}Pb$	$^{206}Pb/^{207}Pb$	$^{206}Pb/^{208}Pb$	$^{207}Pb/^{235}U$	$^{206}Pb/^{238}U$	$^{207}Pb/^{206}Pb$	
Gabbronorite dike at the Kirovogorskoye deposit (1)										
1	0.3	58.7	101.4	2080	5.121	9.961	13.595	0.5193	2741	
2	0.4	48.3	85.0	1600	5.122	10.302	13.300	0.5111	2726	
3	0.3	74.6	142.3	400	4.971	3.161	9.159	0.3888	2566	
4 (bd)	0.3	2.2	33.5	124	6.023	3.002	0.392	0.0530	353	
Siilinjarvi carbonatites (2)										
1 (bd)	1.20	5.8	11.6	1720	5.670	7.319	10.432	0.4386	2550 ± 18	0.73
2	0.50	4.4	8.6	1420	5.483	5.364	10.314	0.4305	2594 ± 60	0.71
3	0.25	4.3	7.0	220	4.308	2.529	9.688	0.3993	2615 ± 60	0.73
4	0.45	1.2	33.6	690	5.124	4.167	1.016	0.0922	2629 ± 30	0.71
Tsaga massif, monzogabbro (3)										
1	1.18	282.9	490.7	17680	5.480	5.482	12.292	0.4904	2669	0.92
2	0.92	370.6	595.3	13700	5.480	4.588	12.918	0.5159	2668	0.94
3	0.65	175.8	288.0	16730	5.487	4.787	12.744	0.5092	2667	0.78
Tsaga massif, labradorite (4)										
18-1	1.00	105.5	179.0	5030	5.464	5.894	12.575	0.5051	2658	0.88
18-2	0.40	186.0	312.7	14560	5.486	5.937	12.686	0.5111	2666	0.67

Continued

18-3	0.25	123.3	204.0	2770	5.421	5.154	12.572	0.5067	2654	0.87
18-4	0.30	345.4	586.3	5340	5.466	5.881	12.579	0.5046	2659	0.88
Borehole C-1, monzonite (5)										
1	2.00	158.9	264.1	6960	5.478	6.188	12.932	0.5178	2660	0.78
2	0.60	198.0	327.5	1860	5.323	6.029	12.872	0.5120	2665	0.95

[1]The ratios are corrected for blanks of 0.08 ng for Pb and 0.04 ng for U and for mass discrimination 0.12% ± 0.04%. [2]Correction for common Pb are determined for the age according to [26].

Table 2. Concentrations of REE in zircons from a gabbronorite dike intersecting the Kirovogorskoye Fe deposit.

Element	Sample No., ppm		
	1	2	3
La	1.42	0.40	0.19
Ce	17.5	13.3	14.6
Pr	0.60	0.20	0.09
Nd	4.22	1.47	1.37
Sm	3.95	2.22	2.05
Eu	0.77	0.54	0.55
Gd	18	11.3	13
Tb	-	-	-
Dy	80.33493	55.76213	56.857
Ho	-	-	-
Er	199	148	169
Tm	-	-	-
Yb	406	325	400
Lu	69.4	53.5	69.2
Total	1099	826	966
$(La/Yb)_n$	0.002518	0.000873	0.000337
$(Eu/Eu^*)_n$	0.24	0.27	0.25
$(Ce/Ce^*)_n$	4.6	11.4	27.4

Table 3. Temperature of the zircon crystallization from a gabbronorite dike intersecting the Kirovogorskoye Fe deposit.

Sample	T1	T2	T3	T_{av}
	800	743	771	771

Table 4. Concentration of REE in zircons from the Tsaga Ti-Mgt deposit.

Element	Sample No.		
	1	2	3
La	23.4	4.58	1.18

Continued

Ce	42	22.2	18.8
Pr	3.45	1.44	3.19
Nd	15.4	5.78	19.1
Sm	2.56	1.32	5.40
Eu	6.93	9.35	4.15
Gd	11.3	10.2	10.3
Tb	-	-	-
Dy	71.8	93.8	66.9
Ho	-	-	-
Er	275	348	277
Tm	-	-	-
Yb	952	1140	955
Lu	153	176	156
Total	1915	2264	1871
$(La/Yb)_n$	0.017590	0.002881	0.000889
$(Eu/Eu^*)_n$	3.34	5.52	1.67
$(Ce/Ce^*)_n$	1.0	2.1	1.6

0.002518). Zircons are rich in Ce, because the value of $(Ce/Ce^*)_N$ varies in the range of 4.6 - 27.4, and poor in Eu, because the value of $(Eu/Eu^*)_N$ is 0.24 - 0.27 [29].

Along with the study of the REE concentrations in zircon crystals, Ti contents and crystallization temperatures of zircon grains have been estimated, using a Ti-in-zircon thermometer [27]. An average temperature of the zircon crystallization in gabbronorites is 771˚C (**Table 3**). This temperature seems to show that zircon formed at the latest stage of the gabbronorite dike crystallization.

Table 4 shows the concentration of REE in zircons from the Tsaga Ti-Mgt deposit. **Figure 4** shows a trend of the REE distribution in zircon from the Tsaga Ti-Mgt deposit. **Table 6** shows the temperature of the zircon crystallization in the Tsaga Ti-Mgt deposit.

Three types of zircon from monzogabbro of the Tsaga Ti-Mgt deposit have been studied, using LA-ICP-MS. The analyzed zircon samples show high total amounts of REE from 1871 to 2264 ppm (**Table 4**). Spectra of the REE distribution in crystal zircons have the same low amount of LREE and high amount of heavy REE. It explains a steep positive incline of the graphs complicated by positive Eu and Ce anomalies, which complies with the trend of the REE distribution in zircon grains of the magmatic origin (**Figure 4**).

Notably, values of $(La/Yb)_N$ are low (0.000889 - 0.017590). It indicates a minor amount of LREE. Zircons are rich in Ce, since the value of $(Ce/Ce^*)_N$ varies in the range of 1.0 - 2.1, and rich in Eu, since the value of $(Eu/Eu^*)_N$ is 1.67 - 5.52 [29].

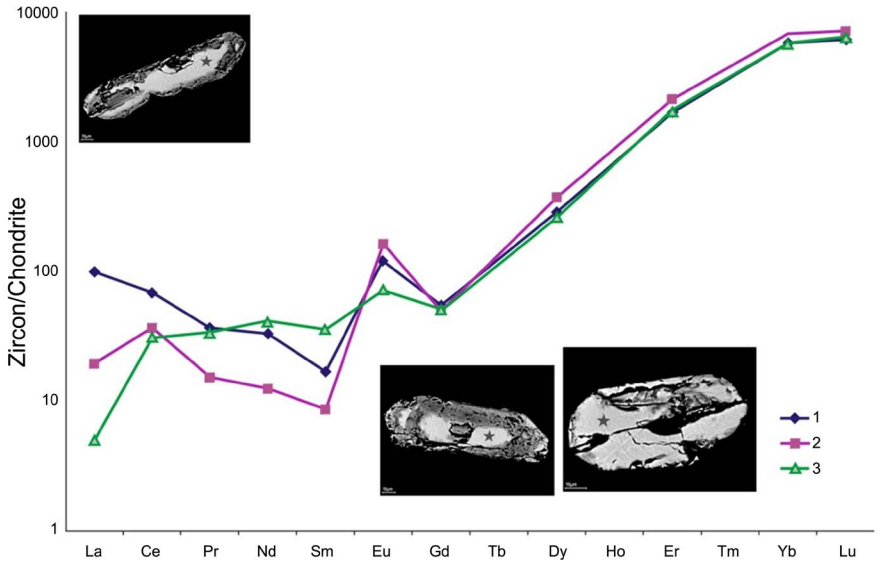

Figure 4. Distribution of REE in zircon from the Tsaga Ti-Mgt deposit [28].

Along with the study of the REE concentrations in zircon crystals, Ti contents and crystallization temperatures of zircon grains have been estimated, using a Ti-in-zircon thermometer. An average temperature of the zircon crystallization in monzogabbro from the Tsaga Ti-Mgt massif is 724˚C (**Table 5**).

Table 6 and **Figure 5** provide data on concentration and distribution of REE in zircons from carbonatites of the Siilinjarvi deposit. **Table 8** shows temperature of the zircon crystallization in the Siilinjarvi deposit.

The precise LA-ICP-MS analysis has been applied to study three types of zircon from carbonatites of the Siilinjarvi deposit. Average total amounts of REE in the zircon grains vary from 33 to 1099 ppm (**Table 7**). LREE are minor, therefore, values of $(Yb/La)_N$ are low (0.000193 - 0.05101). Spectra of the REE distribution have a positive incline of the graphs complicated by positive Eu and Ce anomalies (**Figure 5**). Crystallization temperatures of zircon grains from metagabbro have been estimated, using a Ti-in-zircon thermometer [27]. An average temperature of the U-Pb systematics closure in measured areas of zircon from the Siilinjarvi carbonatites is 646˚C (**Table 7**).

3.2. Baddeleyite in Paleoproterozoic Co-Cu-Ni, Cr-Ti-V-Mgt and PGE Layered Intrusions with Pt-Pd and Cu-Ni Reefs

The formation time of these large igneous provinces (LIPs) is 2.53 Ga to 2.40 Ga, according to U-Pb isotope data (ID-TIMS) on baddeleyite-zircon geochronometer from gabbronorites, anorthosites and dikes cutting the complexes [3] [17] [30].

The Vurechuayvench Pt-Pd reef has been recently discovered within the Monchetundra massif [31]. Its SHRIMP ages are 2501 ± 0.5 Ma on zircon and 2498 ± 1.5 Ma on baddeleyite (**Figures 5-7**). Baddeleyite has been extracted from anorthosites of the middle zone with the Pt-Pd mineralization. New U-Pb (ID-TIMS) analyses yielded ages of 2476 ± 5 Ma and 2471 ± 3 Ma [32].

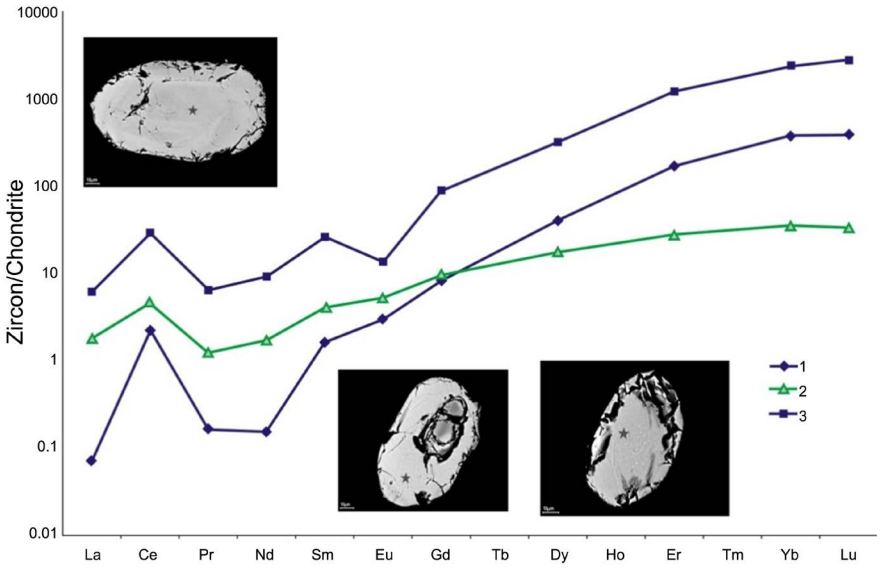

Figure 5. Distribution of REE in zircon from the Siilinjarvi Zr-REE deposit [28].

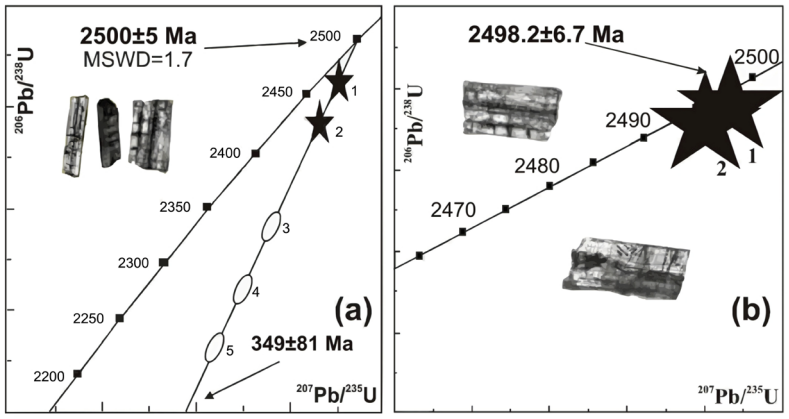

Figure 6. (a) Mt. Nyud, gabbronorite of "critical horizon" (Co-Cu-Ni ores); (b) Vurechuayvench foothills, coarse-grained metagabbronorite (Pt-Pd reef)-Monchegorsk pluton.

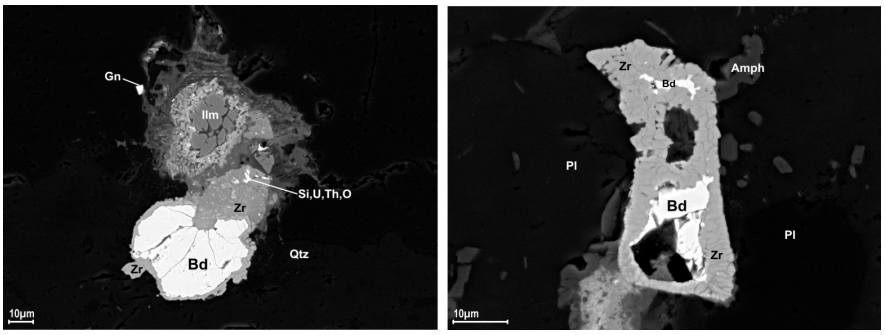

Figure 7. Baddeleyite from Pt-Pd deposits of the Fedorovo-Pana (2.5 Ga) layered intrusion.

Table 5. Temperature of the zircon crystallization, Tsaga Ti-Mgt deposit.

Sample	T1	T2	T3	T_{av}
OG1	784	663	-	724

Table 6. Concentration of REE in zircons from the Siilinjarvi carbonatite deposit.

Element	Sample No.		
	1	2	3
La	0.02	0.42	1.42
Ce	1.35	2.81	17.5
Pr	0.02	0.12	0.60
Nd	0.07	0.79	4.22
Sm	0.24	0.62	3.95
Eu	0.17	0.30	0.77
Gd	1.71	1.97	18
Tb	-	-	-
Dy	9.96	4.37	80.3
Ho	-	-	-
Er	27.7	4.44	199.4
Tm	-	-	-
Yb	61.4	5.87	405.6
Lu	9.74	0.83	69.4
Total	152	33	1099
$(La/Yb)_n$	0.000193	0.05101	0.002518
$(Eu/Eu^*)_n$	0.59	0.76	0.24
$(Ce/Ce^*)_n$	18.9	3.1	4.6

Table 7. Temperature of the zircon crystallization, Siilinjarvi Zr-REE deposit.

Sample	T1	T2	T3	T_{av}
OG1	490	784	663	646

Table 8. U-Pb isotope data for single baddeleyite crystals from coarse-grained metagabbronorite of the Vurechuayvench (Pt-Pd reefs), Monchegorsk pluton.

Sample No.	Weight (mg)	Concentration (ppm)		Pb isotopic composition*			Isotopic ratios**			D,
		Pb	U	$^{206}Pb/^{204}Pb$	$^{206}Pb/^{238}U$	$^{207}Pb/^{235}U$	$^{207}Pb/^{206}Pb$	$^{206}Pb/^{238}U$	$^{207}Pb/^{235}U$	$^{207}Pb/^{206}Pb$	
1 (bd)	0.024	49.847	75.476	1810.2	0.4713 ± 0.0036	10.6714 ± 0.1002	0.16327 ± 0.00088	2499 ± 19	2499 ± 23	2499 ± 13	0
2 (bd)	0.013	95.988	146.99	1419.2	0.4661 ± 0.0042	10.5196 ± 0.1094	0.16337 ± 0.00088	2467 ± 22	2480 ± 25	2498 ± 14	−1.24

*All ratios are corrected for the blank pollution of 1 pg for Pb and 10 pg for U and mass-discrimination of 0.12% ± 0.04%. **Correction for the common lead admixture is determined by age [26]. D is the % discordance. Isotopic ratios are measured on a Finnigan MAT-262 (RPQ) 7-channel mass-spectrometer in the static regime. All errors are given at the level 2 σ. The coordinates of points and parameters of the U-Pb isochron are calculated in the Isoplot program [33] [34], considering commonly accepted decay constants. Baddeleyite is chemically decomposed following the procedure described in [17] [30].

Table 9 provides concentrations of REE, Hf, U, Th and Y in baddeleyite from Paleoproterozoic PGE mafic and Paleozoic alkaline intrusions of the NE Fennoscandian Shield.

Table 9. Estimated concentrations of REE and other elements in grains of baddeleyite from Pt-Pd and Cu-Ni reefs of the Monchegorsk ore area (LA-ICP-MS).

Sample	Grain	Content (average in grain), ppm																			
		Ti	Y	La	Ce	Pr	Nd	Sm	Eu	Gd	Tb	Dy	Ho	Er	Tm	Yb	Lu	Hf	Th	U	ΣREE	T°C
1	2	645	230	0.75	5.65	0.29	2.9	1.52	0.18	5.23	1.51	20.5	8.9	46.8	11.4	107	25.5	4617	2.82	68.2	239	>1000
	3	469	430	12.1	29.4	2.96	16.9	7.08	0.21	18.9	4.72	50.9	17.8	83.1	18.8	162	32.7	2970	9.51	213	458	
	7	1212	849	7.89	39.0	4.19	20.1	10.3	0.41	18.0	4.83	63.8	25.7	156	34.9	315	72	7453	73.8	172	772	
2	4	260	109	0.38	2.11	0.43	1.60	1.58	0.55	3.46	0.88	11.1	4.80	24.6	8.3	69.2	14.5	3060	12.6	58.2	144	
	7-1-4	432	264	1.54	5.35	0.41	2.50	2.45	0.18	5.47	1.94	26.2	9.30	50.1	10.5	94.6	18.1	1413	25.9	89.4	229	
	7-3-4	550	336	1.96	6.80	0.53	3.17	3.11	0.22	6.96	2.47	33.4	11.8	63.8	13.4	120	23.0	1797	32.9	114	291	
	9	879	156	1.95	12.9	1.37	11.5	4.23	0.30	4.94	0.62	11.3	5.85	30.3	5.85	67.1	12.4	5653	31.1	108	171	
3	I 2	1637	21.1	0.09	1.76	0.06	0.41	0.18	0.09	0.54	0.16	1.45	0.69	3.41	0.71	7.22	1.33	6132	2.83	197	18.1	
	II 3	2358	38.6	0.01	3.95	0.01	0.06	0.01	0.02	1.00	0.06	2.49	1.82	6.49	1.48	16.6	3.6	5761	3.04	214	37.6	
	II 2	3949	133	3.88	26.1	0.6	5.96	1.52	2.22	5.58	1.4	14.4	4.19	19.1	4.81	49.1	10.6	10225	27.6	1057	150	
	II 1	940	20.4	0.32	1.56	0.03	0.23	0.13	0.07	0.51	0.19	1.96	0.92	3.9	0.77	6.47	2.16	3068	3.51	136	19.2	
	2-1	6015	52.4	0.20	4.33	0.03	0.57	0.81	0.03	1.12	0.69	6.06	2.34	11.6	2.56	28.2	3.96	17905	13.5	306	62.5	
	1-1	3742	60.6	0.17	4.56	0.04	0.24	0.37	0.14	1.35	0.62	7.18	2.56	12.5	3.04	29.3	4.85	8096	14.7	186	66.9	
	1-3	4876	108	0.60	7.16	0.14	1.2	0.69	0.11	2.81	1.14	10.7	4.84	23.4	6.16	59.8	9.59	17543	10.6	303	128	

Figures 8-10 show average concentrations of REE and normalized chondrites in baddeleyite from gabbronorites and gabbropegmatites of the Monchepluton area.

3.3. Baddeleyite in Paleozoic Complex Deposits

The Paleozoic marked the origin of the largest (Kovdor, Vuoriyarvi, etc.) and super largest (Khibiny and Lovozero) alkaline-subalkaline intrusions with carbonatites.

Baddeleyite has been separated and dated using the U-Pb analysis and LA-ICP-MS. For the first time, the REE distribution and concentrations of Ti and Zr have been studied based on the known temperature of the U-Pb systematics closure (Figure 11(a), Figure 11(b), Table 11). U-Pb, Sm-Nd and Rb-Sr analyses using rocks, accessory and rock-forming minerals from kimberlitic pipes, carbonatites and dike series reflect formation of the biggest mantle reservoirs for primary magma of alkaline-ultra alkaline magmatism in a time span of 465 - 325 Ma (more than 140 Ma) [13] [35]. According to isotope data (ε_{Nd} + 4; I_{Sr} –0.703 - 0.704; T_{Dm} –980 - 700 Ma; enriched by LILE REE; $^3He/^4He$ up to 3.5×10^{-5}) on reference rocks, they originated from the primary mantle reservoirs DM and HIMU [36]. Isotope-geochemical data on U-Pb and LA-ICP-MS dating of baddeleyite from carbonatite and dike complexes suggest that these rocks result from primary magmatic plume activity of Paleozoic magmatism. This magmatism, in its turn, is associated with the break-up of the Pangea supercontinent [37].

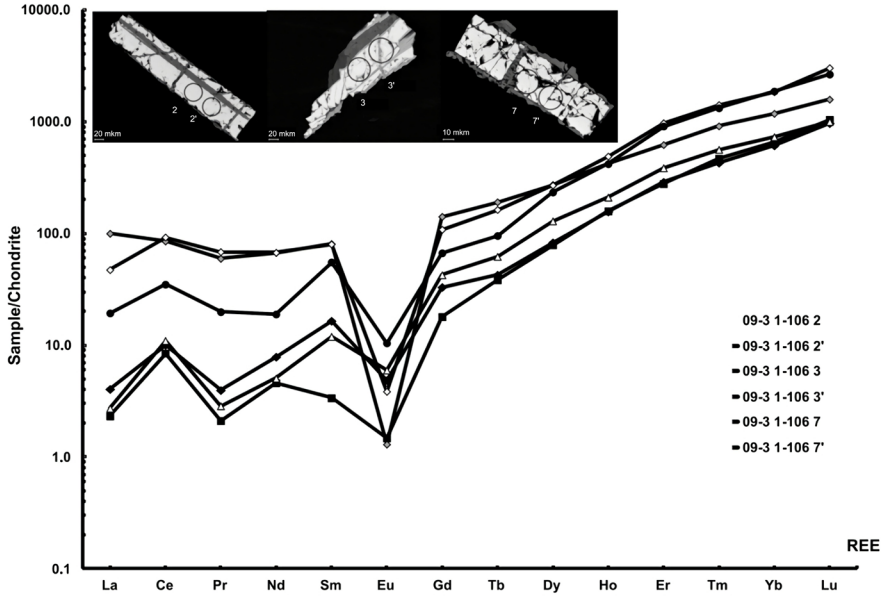

Figure 8. Chondrite normalized REE patterns for baddeleyite from medium-coarse-grained leucogabbronorite with Pt-Pd occurrences (Monchetundra massif) (Sample 1 in **Table 10**) [28].

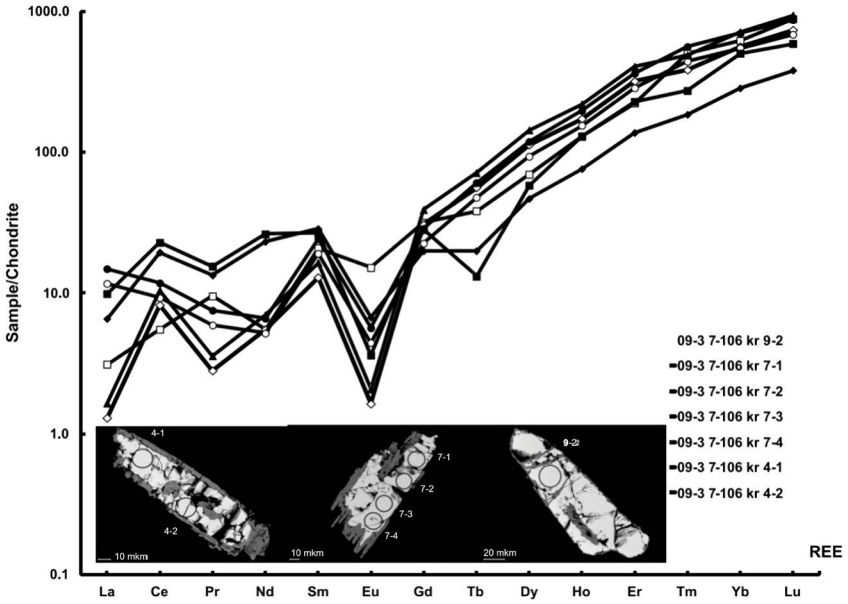

Figure 9. Chondrite normalized REE patterns for baddeleyite from gabbronorite-anorthosite with Pt-Pd occurrences (Monchetundra massif) (Sample 2 in **Table 10**) [28].

Table 10. U-Pb isotope data on baddeleyite (bd) and zircon from the Imandra lopolith and Fedorovo-Pana intrusion.

Sample No.	Weight (mg)	Concentration (ppm)		Pb isotope composition[1)]			Isotope ratios[2)]		Age, Ma[2)]
		Pb	U	$^{206}Pb/^{204}Pb$	$^{206}Pb/^{207}Pb$	$^{206}Pb/^{208}Pb$	$^{207}Pb/^{235}U$	$^{206}Pb/^{238}U$	$^{207}Pb/^{206}Pb$
Anorthosites of the Imandra lopolith									
1034-1 (bd)	1.0	174.6	410.7	6280	6.316	87.0	9.108	0.4219	2419
1034-2 (bd)	0.8	330.6	790.5	14,210	6.351	93.5	9.000	0.4162	2422

Continued

1034-3 (bd)	0.9	457.9	1032.6	28,560	6.334	117.5	9.609	0.4419	2431
Anorthosites of the Fedorovo-Pana intrusion									
P6-1	0.75	218	322	5740	6.230	3.263	11.682	0.5352	2438
P6-2	0.10	743	1331	3960	6.191	3.151	9.588	0.4393	2438
P6-3	0.20	286	577	2980	6.021	3.192	8.643	0.3874	2474
P5 (bd)	1.00	176	396	14,780	6.290	63.610	9.548	0.4380	2435
P6 (bd)	0.26	259	560	3360	6.132	54.950	9.956	0.4533	2443

[1]Ratios are corrected for blanks of 0.08 ng for Pb and 0.04 ng for U and for mass discrimination 0.12% ± 0.04%. [2]Correction for common Pb is determined for the age according to [26].

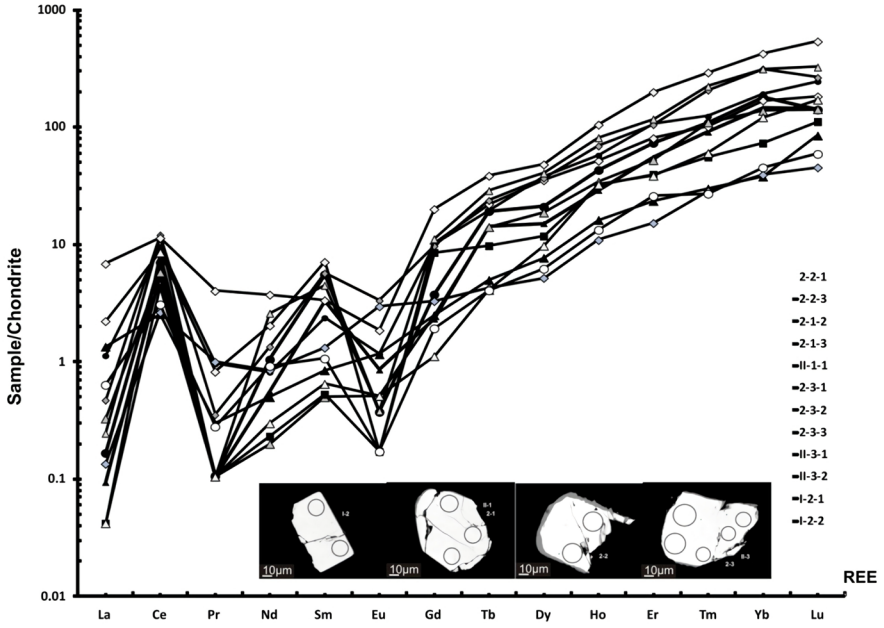

Figure 10. Chondrite normalized REE patterns for baddeleyite from vein pegmatites of the gabbronorite composition (Terrace Cu-Ni deposit, Mt. Nyud) (Sample 3 in **Table 10**) [28].

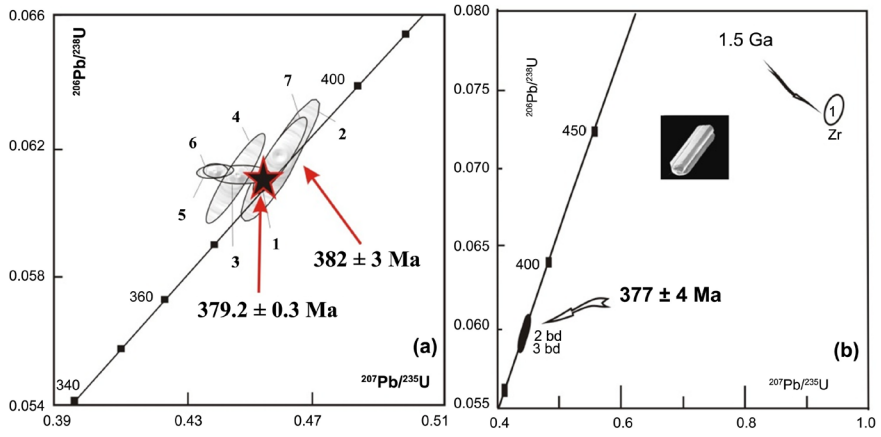

Figure 11. U-Pb isotope data on (a) baddeleyite from foscorite ores in Kovdor; (b) zircon xenocryst (1) from pyroxenite and baddeleyite (2 - 3) from carbonatite of the Vuoriyarvi deposit.

Table 11. U-Pb isotope data on baddeleyite (bd) and zircon (zr) from foscorite ores, Kovdor (1), carbonatites and pyroxenites, Vuorijarvi (2).

Sample No.	Weight (mg)	Concentration (ppm)		Pb isotope composition*			Isotope ratios and age, Ma**			Rho
		Pb	U	$^{206}Pb/^{204}Pb$	$^{206}Pb/^{207}Pb$	$^{206}Pb/^{208}Pb$	$^{207}Pb/^{235}U$	$^{206}Pb/^{238}U$	$^{207}Pb/^{206}Pb$	
Foscorite ores, Kovdor (1)										
1 (bd)	16.80	18.3	318.8	7660	17.88	23.61	0.4541	0.06086	376	
2 (bd)	18.90	9.8	170.3	4790	17.53	44.67	0.4612	0.06194	371	
3 (bd)	29.40	9.2	161.9	4520	17.71	44.11	0.4483	0.06111	338	
4 (bd)	25.00	7.9	139.7	4020	17.66	44.47	0.4457	0.06099	329	
5 (bd)	29.90	9.6	160.9	2920	17.54	50.78	0.4391	0.06123	286	
6 (bd)	30.40	7.6	133.9	3170	17.69	50.75	0.4364	0.06127	281	
7 (bd)	19.90	4.4	73.9	1680	15.89	18.33	0.4584	0.06131	381	
Carbonatites and pyroxenites, Vuorijarvi (2)										
2 (bd)	14.50	4.3	71.9	1220	15.120	12.027	0.442	0.0593	376	0.35
3 (bd)	11.00	6.5	113.3	2840	16.866	19.240	0.447	0.0599	377	0.37
1 (zr)**	8.62	6.7	10.7	670	8.717	0.118	0.951	0.0735	1513	0.48

[1]All ratios are corrected for blanks of 0.08 ng for Pb and 0.04 ng for U and for mass discrimination 0.12% ± 0.04%. [2]Correction for common Pb is determined for the age according to 26]. *Abraded baddeleyite crystals. **Correction is made for the composition of cogenetic galena: $^{206}Pb/^{204}Pb$ = 18.36, $^{207}Pb/^{204}Pb$ = 15.44, $^{208}Pb/^{204}Pb$ = 37.77.

According to new data on the distribution and concentration of REE, Ti and Zr in baddeleyite grains from the Kovdor (**Figure 12**) and Vyoriyarvi (**Figure 13**) massifs measured by LA-ICP-MS (ELAN 9000), the temperature of the U-Pb systematics closure in baddeleyite is higher (984˚C) than that in zircon (–888˚C).

4. Discussion

For the first time, baddeleyite has been defined in Neoarchean rocks of major BIF and Ti-Mgt deposits, Pt-Pd and Cu-Ni reefs of Proterozoic intrusions and Paleozoic complex deposits in the NE Fennoscandian Shield. Since geochronological analysis of baddeleyite is challenging (especially SIMS and SHRIMP) [18] [19] [38], the authors have applied the U-Pb (TIMS) method [3] [13] [17] [30] for precise dating of the above mentioned deposits.

Compared to zircon, baddeleyite is a rarer mineral and a more reliable geochronometer for dating large and superlarge complex deposits using the U-Pb systematics. It is commonly magmatic [2] [39] [40] [41], as opposed to zircon that can be metamorphic, hydrothermal, detritic or occur as xenocrysts. Hence, baddeleyite is much promising for dating of large and superlarge deposits of strategic minerals in the Arctic region.

Isotope U-Pb studies of baddeleyite started in the 1990s. Large (70 - 100 kg) samples have been selected to extract zircon-baddeleyite concentrate for U-Pb

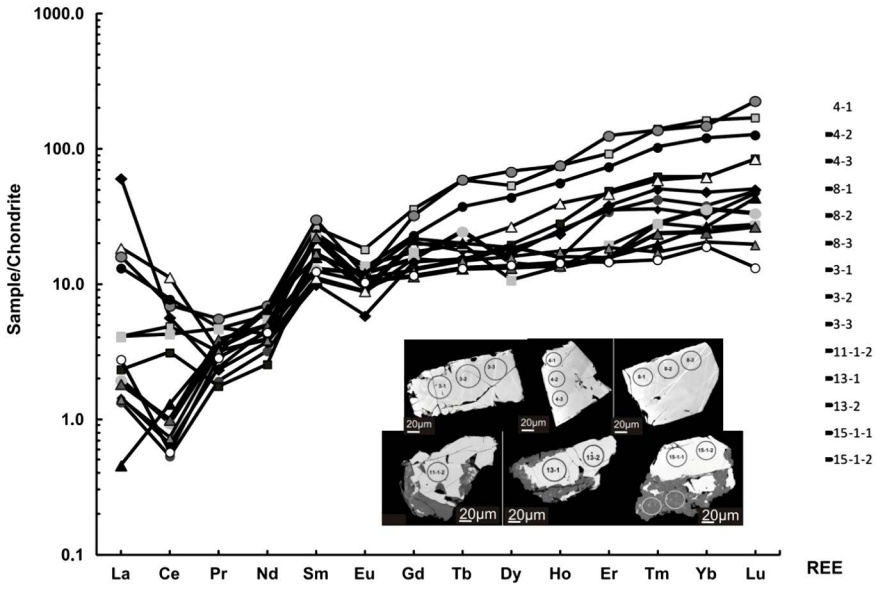

Figure 12. Chondrite normalized REE patterns for baddeleyite from carbonatite of the Vuoriyarvi massif (Sample in **Table 12**) [28].

Table 12. Estimated concentrations of REE and other elements in grains of baddeleyite from carbonatite of the Vuoriyarvi deposit (LA-ICP-MS).

Element	Content (average in grain), ppm										
	5	**4**	**6**	**8**	**3-1**	**1-1**	**7-1**	**10-1**	**11-1-1**	**13-1**	**15-1-1**
Ti	63.6	85.8	120.3	116.8	485.9	82.9	35.4	592.8	74.3	88.2	81.8
Y	4.46	12.0	12.2	23.7	54.5	5.14	3.65	538.1	58.1	7.74	139.7
La	4.22	0.37	5.17	6.44	2.64	0.92	1.78	136.6	2.60	0.27	3.33
Ce	1.90	0.43	5.19	4.09	3.99	0.57	3.78	339.5	7.88	0.70	9.69
Pr	0.16	0.24	0.35	0.23	0.43	0.11	0.45	37.1	1.34	0.35	1.57
Nd	1.57	2.01	1.40	1.59	2.73	2.02	2.38	156.2	10.23	2.69	12.1
Sm	1.53	2.30	1.63	1.95	4.08	1.81	0.77	46.6	7.21	2.92	11.2
Eu	0.32	0.59	0.40	0.46	0.83	0.50	0.33	16.9	2.73	0.66	4.40
Gd	1.67	3.52	1.88	3.24	6.26	1.90	1.21	79.4	14.33	3.39	24.6
Tb	0.39	0.71	0.36	0.63	1.95	0.43	0.19	14.4	2.45	0.62	4.26
Dy	1.91	4.24	2.93	5.45	14.0	2.79	1.01	106.6	13.26	4.03	31.4
Ho	0.47	1.02	0.77	1.72	3.91	0.63	0.23	24.4	2.66	0.84	6.93
Er	1.42	4.71	3.35	7.40	16.1	2.08	1.01	69.1	8.42	2.60	19.9
Tm	0.36	0.90	0.61	1.46	3.25	0.32	0.14	9.33	1.01	0.55	2.76
Yb	3.16	6.02	6.24	9.78	24.5	2.11	0.81	55.7	6.27	4.33	16.6
Lu	0.51	1.09	0.97	1.86	4.45	0.46	0.34	7.26	1.03	0.89	2.24
Hf	3072	3721	5809	7628	18072	1040	859	3866	1287	1318	3149
Th	2.60	1.35	2.66	4.87	4.82	0.72	0.30	1011	119.4	1.15	158.8
U	3.16	12.9	7.18	30.7	38.4	6.06	1.89	85.7	4.4	7.07	3.30
ΣREE	**18.5**	**27.2**	**30.9**	**45.2**	**88.4**	**16.6**	**14.4**	**1099.0**	**81.4**	**24.8**	**151.0**
T˚C	950˚C - 1000˚C										

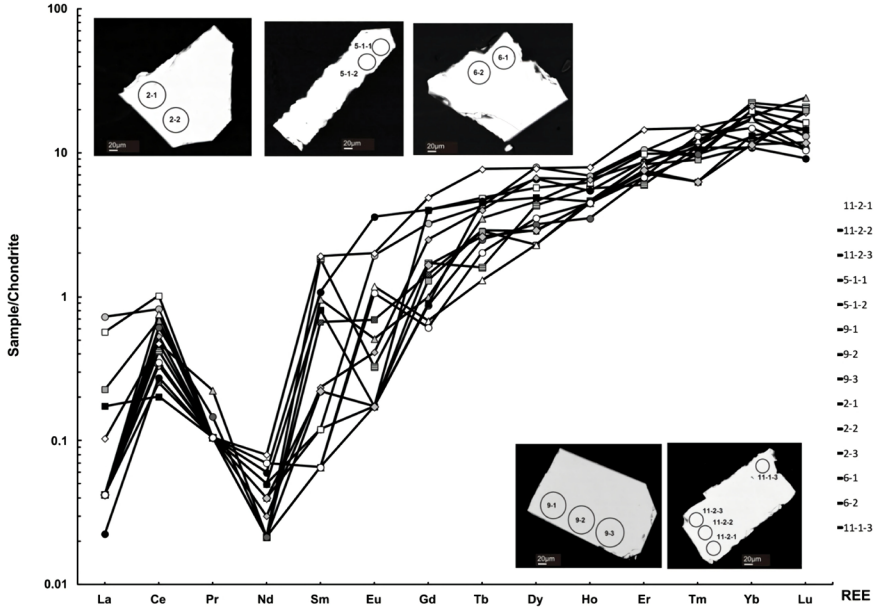

Figure 13. Chondrite normalized REE patterns for baddeleyite from carbonatite of the Kovdor deposit (Sample in **Table 13**) [28].

Table 13. Estimated concentrations of REE and other elements in grains of baddeleyite from carbonatite of the Kovdor deposit (LA-ICP-MS).

Element	Content (average in grain), ppm													
	5-1	9	6	2	11-1	11-2	5 pr	1 pr	1	3	4	5-2	10	11
Ti	34.8	23.5	18.1	12.4	16.5	21.7	34.9	54.7	55.0	37.2	39.2	91,0	33.8	18.0
Y	8.07	6.30	3.68	5.70	5.60	6.64	2.40	8.70	4.50	4.20	2.37	24.8	11.9	4.80
La	0.11	0.01	0.10	0.02	0.01	0.01	0.26	0.24	0.04	0.14	0.11	0.07	0.09	0.04
Ce	0.66	0.26	0.23	0.42	0.28	0.23	0.28	0.45	0.3	0.27	0.16	1.36	0.68	0.19
Pr	0.02	0.01	0.07	0.01	0.01	0.01	0.14	0.10	0.37	0.15	0.08	0.06	0.05	0.04
Nd	0.02	0.03	0.02	0.01	0.11	0.01	0.93	0.77	0.58	0.28	0.21	0.68	0.21	0.07
Sm	0.06	0.16	0.06	0.02	0.03	0.18	2.35	1.51	1.42	0.63	0.18	0.5	0.72	0.34
Eu	0.04	0.12	0.01	0.03	0.03	0.03	0.40	0.24	0.38	0.49	0.08	0.17	0.20	0.04
Gd	0.72	0.78	0.24	0.19	0.22	0.28	2.56	1.66	1.21	2.43	0.51	1.25	1.24	0.26
Tb	0.20	0.20	0.15	0.08	0.12	0.10	0.43	0.43	0.29	0.50	0.10	0.31	0.24	0.12
Dy	1.65	1.78	0.94	0.66	0.97	1.00	1.50	2.40	1.32	3.12	0.64	2.27	2.04	0.86
Ho	0.37	0.38	0.25	0.24	0.26	0.32	0.31	0.47	0.29	0.55	0.14	0.77	0.63	0.21
Er	1.94	1.76	1.23	1.29	1.27	1.31	1.03	2.64	1.62	1.50	0.48	3.36	2.12	0.77
Tm	0.28	0.32	0.18	0.26	0.25	0.32	0.36	0.61	0.36	0.29	0.07	0.48	0.43	0.15
Yb	3.01	2.48	1.97	2.33	2.28	3.24	1.47	4.08	1.93	1.7	0.5	4.9	3.44	1.06
Lu	0.37	0.4	0.31	0.38	0.33	0.47	0.35	0.67	0.33	0.43	0.12	0.97	0.77	0.18
Hf	4834	5335	7330	7390	6445	7752	1916	11517	1386	1541	1025	8096	1849	2167
Th	4.4	1.45	0.36	1.01	0.52	0.62	0.84	1.26	0.8	0.57	0.26	5.16	4.48	0.45
U	35.1	13.8	5.57	22.6	8.5	10.2	5.3	18.9	5.18	9.3	3.2	62	59.7	13.9
ΣREE	8.91	6.6	3.4	5.9	6.04	7.46	12.3	16.3	9.74	9.32	2.83	17.2	12.6	3.86

studies. The article provides U-Pb data on baddeleyite (2738 ± 6 Ma) from a gabbronorite dike intersecting ores of the Olenegorskoye BIF [9]. Nowadays, the most ancient U-Pb age on baddeleyite (2.7 Ga) is known for the Stillwater PGE deposit only [42] and equals U-Pb data to baddeleyite from the Olenegorskoye BIF. U-Pb isotope data on baddeleyite have been recently obtained and compared to zircon ages [43]. The youngest Paleozoic age is estimated on baddeleyite from the Kovdor foscorite-baddeleyite deposit (380 - 348 Ma). Thus, baddeleyite is studied in the eastern Baltic Shield for the period of 2.7 Ga to 348 Ma, *i.e.* for the time span of more than 2.4 Ga.

LA-ICP-MS has been first applied to study concentrations and distributions of REE in baddeleyite from the deposits. Studying and applying Zr-Ti geochronometer for baddeleyite is considered important. New investigations yield higher temperatures of the baddeleyite grains formation and the U-Pb systematics closure (more than 10,000˚C), compared to zircon (less than 9000˚C) [20] [21] [22]. These newly obtained high temperatures of the U-Pb systematics closure and baddeleyite formation are close to other geochronometers, e.g. pyroxenes from mafic rocks, but require further study.

The content of Ti in grains varies widely. It is 10 - 37 ppm (21.2 on average) for sample Bd-300 and 28 - 72 ppm (44.8 on average) for sample Bd-300 (prismatic), 47 - 150 ppm (96.6 on average) for sample Bd-400 and 0.31% - 0.79% (0.49% on the average) for older baddeleyite M-2.

Average temperatures of the baddeleyite crystallization and U-Pb system closure have been detected using a zircon-applied method [27]. Ti-in-zircon thermometer has never been used for baddeleyite before. We apply this method for the first time as a test to check how it works for baddeleyite. They are calculated at 804˚C - 888˚C for Kovdor and 984˚C for Vuoriyarvi. Notably, baddeleyite from the Monchegorsk pluton has high crystallization temperatures of more than 1000˚C (**Table 6**).

Isotope-geochemical data based on Nd-Sr-He systematics for the rocks of PGE layered Paleoproterozoic intrusions and Ilm and Mgt minerals suggest the mantle impact of N-MORB, E-MORB and OIB sources to dike complexes [3] [17] [30] [32]. Primary-mantle protolith is characterized by εNd 1 - 3; ISr 0.702 - 0.704; TDm 3.5 - 2.8 Ga; enriched by LILE REE elements; 3He/4He up to 1.5×10^{-6}. Re-Os investigations suggest the plume origin of an enriched mantle reservoir EM-1 [Yang 2016]. Cu-Ni-Cr-Ti-V-Fe and PGE deposits formed in the Kola province owing to the large plume magmatism and probably the break-up of the oldest Kenorland supercontinent [3] [14] [17].

5. Conclusions

Baddeleyite has been sampled from important industrial deposits in the Arctic region and reference rocks of the Neoarchean BIF, Paleoproterozoic Cu-Ni and Pt-Pd layered intrusions, as well as Paleozoic alkaline and ultra-alkaline ore deposits. Analyses of the sampled minerals have indicated their primary magmatic

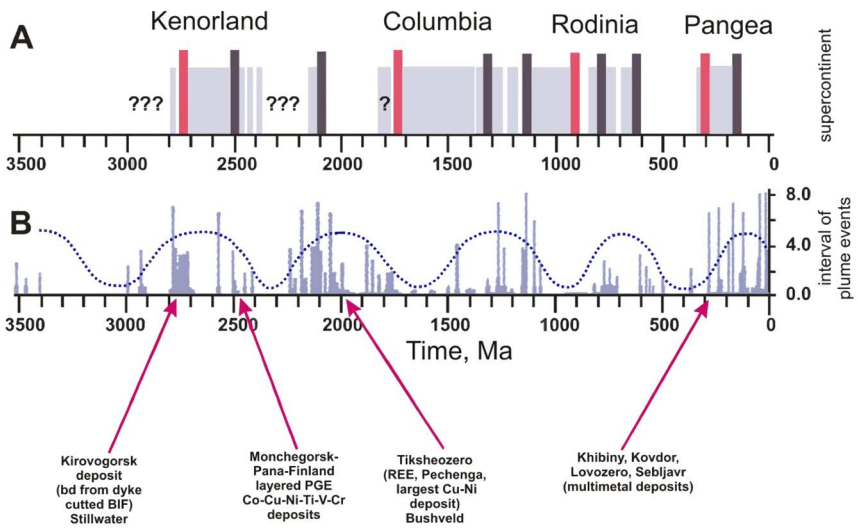

Figure 14. Correlation of supercontinental cycles (a) with a period of 750 - 900 Ma for the mantle-plume (b) activity.

genesis. In terms of the U-Pb geochronology, baddeleyite is important in indicating the formation time and duration of magmatic activity. It is also crucial for the reconstruction of supercontinents.

Based on new precise U-Pb data on baddeleyite, we can assume that the major deposits formed in periods of the plume activity (**Figure 14(b)**). They, in turn, correlate with supercontinental cycles, as shown in **Figure 14(a)**.

This article pioneers in linking the break-up of supercontinents and baddeleyite, which is used as a basis for paleo-reconstructions of the continents [7] [37] [44]. For the first time, this paper provides a modeled link between the break-up of supercontinents and complex deposits with baddeleyite, since all complex deposits are derivates of LIPs from the Archean to Paleozoic [45].

Author Contributions

Conceptualization, T.B.; Methodology, T.B., S.D. and A.N.; Validation, T.B., E.S.; Formal Analysis, T.B., V.S., S.D. and A.N.; Investigation, T.B., V.S., S.D., A.N. and E.S.; Writing-Original Draft Preparation, T.B., E.S.; Writing-Review & Editing, T.B., A.N., S.D. and E.S.; Supervision, T.B.

Funding

The research has been carried out in the framework of the scientific research contract No. 0226-2019-0053, grants RFBR 18-35-00246, 18-05-70082 and Program by Presidium RAS No. 8.

Acknowledgements

This paper is dedicated to Academician F.P. Mitrofanov, who initiated baddeleyite studies in the Pt-bearing province in the Arctic region of the NE Fennoscandian Shield.

Conflicts of Interest

The authors declare no conflict of interest.

References

[1] Heaman, L.M. and Le Cheminant, A.N. (1993) Paragenesis and U-Pb Systematics of Baddeleyite (ZrO). *Chemical Geology*, **110**, 95-126. https://doi.org/10.1016/0009-2541(93)90249-I

[2] Corfu, F., Bayanova, T., Shchiptsov, V. and Frantz, N. (2011) A U-Pb ID-TIMS Age of the Tiksheozero Carbonatite: Expression of 2.0 Ga Alkaline Magmatism in Karelia, Russia. *Central European Journal of Geosciences*, **3**, 302-308. https://doi.org/10.2478/s13533-011-0029-z

[3] Bayanova, T., Ludden, J. and Mitrofanov, F. (2009) Timing and Duration of Paleoproterozoic Events Producing Ore-Bearing Layered Intrusions of the Baltic Shield: Metallogenic, Petrological and Geodynamic Implications. In: Reddy, S.M., Mazumder, R., Evans, D.A.D. and Collins, A.S., Eds., *Paleoproterozoic Supercontinents and Global Evolution*, Geological Society, Special Publications, London, Volume 323, 165-198. https://doi.org/10.1144/SP323.8

[4] Reischmann, T., Brugmann, G.E., Jochum, K.P. and Todt, W.A. (1995) Trace Element and Isotopic Composition of Baddeleyite. *Mineral Petrology*, **53**, 155-164. https://doi.org/10.1007/BF01171953

[5] Van Kranendonk, M.J., Bennett, V.C. and Hoffmann, J.E. (2019) Earth's Oldest Rocks. Elsevier, Amsterdam, 1112.

[6] Bayanova, T.B., Kunakkuzin, E.L., Serov, P.A., Fedotov, D.A., Borisenko, E.S., Elizarov, D.V. and Larionov, A.V. (2016) Precise U-Pb (ID-TIMS) and SHRIMP-II Ages on Single Zircon and Nd-Sr Signatures from Achaean TTG and High Aluminum Gneisses on the Fennoscandian Shield. *Proceedings of the* 32*nd Nordic Geological Winter Meeting*, Helsinki, 13-15 January 2016, 172.

[7] Bleeker, W. (2003) The Late Archean Record: Puzzle in ca. 35 Pieces. *Lithos*, **71**, 99-134. https://doi.org/10.1016/j.lithos.2003.07.003

[8] Mutanen, T. and Huhma, H. (2003) The 3.5 Ga Siurua Trondhjemite Gneiss in the Archean Pudas-Jarvi Granulite Belt, Northern Finland. *Bulletin of the Geological Society of Finland*, **75**, 51-68. https://doi.org/10.17741/bgsf/75.1-2.004

[9] Bayanova, T.B., Mitrofanov, F.P. and Egorov, D.G. (1998) U-Pb Dating of the Dike Complex at the Kirovogorsk Deposit in the Iron Ore Formation of the Kola Peninsula. *Doklady Earth Sciences*, **361**, 688-691.

[10] Mitrofanov, F.P., Zozulya, D.R., Bayanova, T.B. and Levkovich, N.V. (2000) The World's Oldest Anorogenic Alkali Granitic Magmatism in the Keivy Structure on the Baltic Shield. *Doklady Earth Sciences*, **374**, 1145-1148.

[11] Zozulya, D.R., Bayanova, T.B. and Nelson, E.G. (2005) Geology and Age of the Late Archean Keivy Alkaline Province, Northeastern Baltic Shield. *Journal of Geology*, **113**, 601-608. https://doi.org/10.1086/431912

[12] Poutiainen, M. (1995) Fluids in the Siilinjärvi Carbonatite Complex, Eastern Finland: Fluid Inclusion Evidence for the Formation Conditions of Zircon and Apatite. *Bulletin of the Geological Society of Finland*, **67**, 3-18. https://doi.org/10.17741/bgsf/67.1.001

[13] Bayanova, T.B. (2006) Baddeleyite: A Promising Geochronometer for Alkaline and Basic Magmatism. *Petrology*, **14**, 187-200. https://doi.org/10.1134/S0869591106020032

[14] Mitrofanov, F.P., Bayanova, T.B. and Korchagin, A.U. (2013) East Scandinavian and Noril'sk Plume Mafic Large Igneous Provinces of Pd-Pt Ores: Geological and Metallogenic Comparison. *Geology of Ore Deposits*, **55**, 305-319. https://doi.org/10.1134/S107570151305005X

[15] Mints, M.V., Sokolova, E.Yu., Glaznev, V.N. and LADOGA Work Team (2017) 3D Model of Deep Structure of the Svecofennian Accretion Orogen (Finland, Russia): Synthesis of Data on Geological Mapping, Seismic Profiling, Metal Tellurics and Proceedings of the Scientific Conference and Guidebook on Scientific Excursions. Geodynamics of the Early Precambrian: Common and Distinguish Features with the Phanerozoic. Karelian Scientific Centre RAS, Petrozavodsk, 179-184.

[16] Mitrofanov, F.P. (1996) Geological Map of the Kola Region. Scale 1:500000. Regional Geophysics Lab., GI KSC RAS, GIS ArcView 3.0.

[17] Bayanova, T., Mitrofanov, F., Serov, P., Nerovich, L., Yekimova, N., Nitkina, E. and Kamensky, I. (2014) Layered PGE Paleoproterozoic (LIP) Intrusions in the NE Part of the Fennoscandian Shield—Isotope Nd-Sr and 3He/4He Data Summarizing U-Pb Ages (on Baddeleyite and Zircon), Sm-Nd Data (on Rock-Forming and Sulphide Minerals), Duration and Mineralization. In: Mörner, N.-A., Ed., *Geochronology—Methods and Case Studies*, INTECH, London, 143-193. https://doi.org/10.5772/58835

[18] Schmitt, A.K., Chamberlain, K.R., Swapp, S.M. and Harrison, T.M. (2010) *In Situ* U-Pb Dating of Micro-Baddeleyite by Secondary Ion Mass Spectrometry. *Chemical Geology*, **269**, 386-395. https://doi.org/10.1016/j.chemgeo.2009.10.013

[19] Li, Q.-L., Li, X.-H., Liu, Y., Tang, G.-Q., Yanga, J.-H. and Zhu, W.-G. (2010) Precise U-Pb and Pb-Pb Dating of Phanerozoic Baddeleyite by SIMS with Oxygen Flooding Technique. *Journal of Analytical Atomic Spectrometry*, **25**, 1107-1113. https://doi.org/10.1039/b923444f

[20] Nikolaev, A.I., Drogobuzhskaya, S.V., Bayanova, T.B., Kaulina, T.V., Lyalina, L.M., Novikov, A.I. and Steshenko, E.N. (2016) REE Distribution in Zircon from Reference Rocks of the Arctic Region: Evidence from Study by the LA-ICP-MS Method. *Doklady Earth Sciences*, **470**, 1037-1041. https://doi.org/10.1134/S1028334X16100044

[21] Steshenko, E.N., Nikolaev, A.I., Bayanova, T.B., Drogobuzhskaya, S.V., Chashchin, V.V., Serov, P.A., Lyalina, L.M. and Novikov, A.I. (2017) The Paleoproterozoic Kandalaksha Anorthosite Massif: New U-Pb (ID-TIMS) Data and Geochemical Features of Zircon. *Doklady Earth Sciences*, **477**, 1454-1457. https://doi.org/10.1134/S1028334X17120194

[22] Steshenko, E.N., Nikolaev, A.I., Bayanova, T.B., Drogobuzhskaya, S.V., Chashchin, V.V., Serov, P.A., Lyalina, L.M., Novikov, A.I. and Elizarov, D.V. (2018) The Paleoproterozoic Kolva Anorthosite Block: New Data on the U-Pb Age (ID TIMS) and Geochemical Features of Zircon. *Doklady Earth Sciences*, **479**, 366-370. https://doi.org/10.1134/S1028334X18030224

[23] NIST (2012) Certificate of Analysis. Standard Reference Material 612. Trace Element in Glass. 1-4.

[24] Pearce, N.J.G., Perkins, W.T. and Westgate, J.A. (1997) A Compilation of New and Published Major and Trace Element Data for NIST SRM 610 and NIST SRM 612 Glass Reference Materials. *Geostandards Newsletter*, **21**, 115-144. https://doi.org/10.1111/j.1751-908X.1997.tb00538.x

[25] Jochum, K.P., Weis, U., Stoll, B., Kuzmin, D., Yang, Q., Raczek, I., Jacob, D.E., Stracke, A., Birbaum, K., Frick, D.A., Günther, D. and Enzweiler, J. (2011) Deter-

mination of Reference Values for NIST SRM 610-617 Glasses Following ISO Guidelines. *Geostandards and Geoanalytical Research*, **35**, 397-429. https://doi.org/10.1111/j.1751-908X.2011.00120.x

[26] Stacey, J.S. and Kramers J.D. (1975) Approximation of Terrestrial Lead Isotope Evolution by a Two-Stage Model. *Earth and Planetary Science Letters*, **26**, 207-221. https://doi.org/10.1016/0012-821X(75)90088-6

[27] Watson, E.B., Wark, D.A. and Thomas, J.B. (2006) Crystallization Thermometers for Zircon and Rutile. *Contributions to Mineralogy and Petrology*, **151**, 413-433. https://doi.org/10.1007/s00410-006-0068-5

[28] Sun, S.S. and McDonough, W.F. (1989) Chemical and Isotopic Systematics of Oceanic Basalts; Implications for Mantle Composition and Processes. In: Saunders, A.D. and Norry, M.J., Eds., *Magmatism in Ocean Basins*, Geol. Soc. London, London, Volume 42, 313-345. https://doi.org/10.1144/GSL.SP.1989.042.01.19

[29] Hoskin, P.W.O. and Schaltegger, U. (2003) The Composition of Zircon and Igneous and Metamorphic Petrogenesis. *Zircon*: *Reviews in Mineralogy and Geochemistry*, **53**, 27-62. https://doi.org/10.2113/0530027

[30] Bayanova, T., Korchagin, A., Mitrofanov, A., Serov, P., Ekimova, N., Nitkina, E., Kamensky, I., Elizarov, D. and Huber, M. (2019) Long-Lived Mantle Plume and Polyphase Evolution of Paleoproterozoic PGE Intrusions in the Fennoscandian Shield. *Minerals*, **9**, 1-22. https://doi.org/10.3390/min9010059

[31] Rundkvist, T.V., Bayanova, T.B., Sergeev, S.A., Pripachkin, P.V. and Grebnev, R.A. (2014) The Paleoproterozoic Vurechuayvench Pt-Bearing Layered Massif (Kola Peninsula): New Results of U-Pb (ID-TIMS and SHRIMP) Dating of Baddeleyite and Zircon. *Doklady RAS*, **454**, 67-72. https://doi.org/10.1134/S1028334X14010048

[32] Nerovich, L.I., Bayanova, T.B., Serov, P.A. and Elizarov, D.V. (2014) Magmatic Sources of Dikes and Veins of the Monchetundra Massif (Baltic Shield): Results of Isotope-Geochronological and Geochemical Research. *Geokhimiya*, **7**, 605-624. https://doi.org/10.1134/S0016702914070052

[33] Ludwig, K.R. (1991) PBDAT—A Computer Program for Processing Pb-U-Th Isotope Data. Version 1.22. Open-File Report 88-542, U.S. Geological Survey, Reston, 38.

[34] Ludwig, K.R. (1999) ISOPLOT/Ex—A Geochronological Toolkit for Microsoft Excel. Version 2.05. Berkeley Geochronology Center Special Publication, Berkeley, Volume 1a, 49.

[35] Rodionov, N.V., Antonov, A.V., Kapitonov, I.N., Sergeev, S.A. and Belyatsky, B.V. (2012) Comparative *In-Situ* U-Th-Pb Geochronology and Trace Element Composition of Baddeleyite and Low-U Zircon from Carbonatites of the Paleozoic Kovdor Alkaline-Ultramafic Complex, Kola Peninsula, Russia. *Gondwana Research*, **21**, 728-744. https://doi.org/10.1016/j.gr.2011.10.005

[36] Tolstikhin, I.N., Kamensky, I.L., Marty, B., Nivin, V.A., Vetrin, V.R., Balaganskaya, E.G., Ikorsky, S.V., Gannibal, M.A., Kirnarsky, Yu.M., Weiss, D., Verhulst, A. and Demaffe, D. (1999) Identification of Substances of the Lower Mantle Plume in the Devonic-Alkaline-Ultrabasic-Carbonatite Complexes Ring Peninsulas Based on the Study of Isotopy of Noble Gas and Radioactive Elements. Apatity-Nancy-Brussels: Kola Science Center, Russian Academy of Sciences, National Center for Scientific Research, France, Free University of Brussels, Belgium, 97 p.

[37] Lubnina, N.V. (2009) East-European Craton from Neoarhaean to Paleozoic Time Based on Paleomagnetic Data. Dr. Thesis Manuscript, MSU, Moscow.

[38] Wingate, M.T.D. and Compston, W. (2000) Crystal Orientation Effects during Ion

Microprobe U-Pb Analysis of Baddeleyite. *Chemical Geology*, **168**, 75-97. https://doi.org/10.1016/S0009-2541(00)00184-4

[39] Krogh, T.E., Davis, D.W. and Corfu, F. (1984) Precise U-Pb Zircon and Baddeleyite Ages for the Sudbury Area. In: Pye, E.G., Naldrett, A.J. and Giblin, P.E., Eds., *The Geology and Ore Deposits of the Sudbury Structure*, Ontario Geological Survey, Specifications Vol. 1, Sudbury, 431-446.

[40] Heaman, L.M. and Tarney, I. (1989) U-Pb Baddeleyite Ages for the Scourie Dyke Swarm, Scotland: Evidence for Two Distinct Intrusion Events. *Nature*, **3**, 703-705. https://doi.org/10.1038/340705a0

[41] Rioux, M., Bowring, S., Dudas, F. and Hanson, R. (2010) Characterizing the U-Pb Systematics of Baddeleyite through Chemical Abrasion: Application of Multi-Step Digestion Methods to Baddeleyite Geochronology. *Contributions to Mineralogy and Petrology*, **160**, 777-801. https://doi.org/10.1007/s00410-010-0507-1

[42] Wall, C.J., Scoates, J.S., Weis, D., Friedman, R.M., Amini, M. and Meurer, W.P. (2018) The Stillwater Complex: Integrating Zircon Geochronological and Geochemical Constraints on the Age, Emplacement History and Crystallization of a Large, Open-System Layered Intrusion. *Journal of Petrology*, **59**, 153-190. https://doi.org/10.1093/petrology/egy024

[43] Mungall, J., Kamo, S.L. and McQuade, S. (2016) U-Pb Geochronology Documents Out-of-Sequence Emplacement of Ultramafic Layers in the Bushveld Igneous Complex of South Africa. *Nature Communications*, **7**, Article No. 13385. https://doi.org/10.1038/ncomms1338

[44] Li, Z.X., Bogdanova, S.V., Collins, F.S., Davidson, A., De Waele, B., Ernst, R.E., Fitzsimons, I.C.W., Gladkochub, D.P., Jacobs, J., Karlstrom, K.E., Lu, S., Natapov, L.M., Pease, V., Pisarevsky, S.A., Thrane, K. and Vernikovsky, V. (2008) Assembly, Configuration, and Break-Up History of Rodinia: A Synthesis. *Precambrian Research*, **160**, 179-210. https://doi.org/10.1016/j.precamres.2007.04.021

[45] Ernst, R.E. (2014) Large Igneous Provinces. Cambridge University Press, Cambridge, 666. https://doi.org/10.1017/CBO9781139025300